

9783

NACA TN 3500

0066620



TECH LIBRARY KAFB, NM

NATIONAL ADVISORY COMMITTEE FOR AERONAUTICS

TECHNICAL NOTE 3500

CORRECTION OF ADDITIONAL SPAN LOADINGS COMPUTED BY THE
WEISSINGER SEVEN-POINT METHOD FOR MODERATELY
TAPERED WINGS OF HIGH ASPECT RATIO

By John DeYoung and Walter H. Barling, Jr.

Ames Aeronautical Laboratory
Moffett Field, Calif.



Washington
July 1955

AFM2C

TECHNICAL NOTE
3500



NATIONAL ADVISORY COMMITTEE FOR AERONAUTICS

TECHNICAL NOTE 3500

CORRECTION OF ADDITIONAL SPAN LOADINGS COMPUTED BY THE
WEISSINGER SEVEN-POINT METHOD FOR MODERATELY
TAPERED WINGS OF HIGH ASPECT RATIO

By John DeYoung and Walter H. Barling, Jr.

SUMMARY

It has been found that for wings combining high aspect ratio with large amounts of sweep, the Weissinger seven-point results are in error. A simple procedure is presented here which for a sizable range of plan forms largely corrects these errors and results in more accurate span loadings being read directly from the loading charts of NACA Report 921. This procedure consists of an alteration of the taper ratio used plus an additional correction applied at the wing root. In the above procedure, the lift-curve slope and the method of fairing the loading are also improved.

The new results agree within ± 1 percent with theoretical results believed to be accurate; whereas maximum errors of the original Weissinger seven-point loading (for wings swept back 45°) are approximately 2 and 8 percent for aspect ratios equal to 3 and 10, respectively.

INTRODUCTION

Of the several published methods for computing the span loading of wings at subsonic speeds, the Weissinger "L" method with seven control points across the span is one of the easier methods to use and, at one time, appeared to afford the best compromise between labor and accuracy. Solutions for many wings have been plotted (ref. 1). The mathematical coefficients, a_{vn} , used in the four equations have also been presented in graphical form for plan forms whose solutions are not plotted.

Garner (ref. 2), Schneider (ref. 3), and others have indicated that for wings combining high aspect ratio with large amounts of sweepback, the seven-point loadings do not compare favorably with experimental results nor with theoretical results believed to be more accurate. The seven-point Weissinger loadings, $c_l c / C_{L_{cav}}$, are generally too high outboard and too low inboard, as is illustrated in figure 1 (taken from ref. 3).

The primary purpose of the present report is to find some simple, direct corrections to the solutions given in reference 1 for sweptback wings of high aspect ratio.

NOTATION

A	aspect ratio, $\frac{b^2}{S}$
a_{vn}	coefficients relating the wing loading at station n to the downwash at station v
b	wing span measured perpendicular to the plane of symmetry, ft
c	local wing chord measured parallel to the plane of symmetry, ft
c_{av}	average wing chord, $\frac{S}{b}$, ft
C_L	lift coefficient, $\frac{\text{total lift}}{qS}$
$C_{L\alpha}$	lift-curve slope, per radian or deg
c_l	section lift coefficient
$c_{l\alpha}$	section lift-curve slope, per radian or deg
G	spanwise loading coefficient or dimensionless circulation, $\frac{c_l c}{2b}$ or $\frac{\Gamma}{bV}$
k	constants to be evaluated in the aspect-ratio-reduction functions
K	equal to $\frac{c_l c}{C_L c_{av}}$, $K = \frac{2AG}{C_L}$
M_∞	free-stream Mach number
M	number of terms used in a numerical integration to obtain a_{vn}
m	number of points across the wing span at which the downwash is determined and the boundary conditions satisfied; also the coefficient of ϕ in the last term of the trigonometric loading series
q	free-stream dynamic pressure, lb/sq ft
R	Reynolds number based on mean aerodynamic chord

S	wing area, sq ft
V	free-stream velocity, ft/sec
α	wing angle of attack, radians
Γ	circulation, ft ² /sec
γ	a correction term to take into account errors in a four-term numerical integration of span loadings, G_n , to obtain lift
η	dimensionless lateral coordinate, $\frac{y}{b/2}$
Λ	sweep angle of the wing quarter-chord line, positive for sweepback, deg
Λ_p	sweep angle resulting from the Prandtl-Glauert transformation, $\Lambda_p = \tan^{-1} \frac{\tan \Lambda}{\sqrt{1 - M_o^2}}$
λ	geometric wing taper ratio, $\frac{\text{tip chord}}{\text{root chord}}$
λ_e	an effective taper ratio which results in more accurate answers being read from the loading charts of reference 1
σ	a correction term to increase lift in the vicinity of $\eta = 0$
ϕ	trigonometric spanwise coordinate, $\cos^{-1} \eta$, radians

Subscripts

n	number pertaining to span station associated with the loading, $\eta_n = \cos(n\pi/m + 1)$
ν	number pertaining to span station associated with the downwash, $\eta_\nu = \cos(\nu\pi/m + 1)$
7	values given by the procedure of reference 1

DEVELOPMENT OF CORRECTIONS

Outline of Development

In the material to follow, the mathematical errors resulting from seven-point solutions will be approximately corrected by an effective change in wing taper ratio, the addition of a term to the loading at the

wing root, and a correction to the total lift. All corrections will be based on the easily determined errors of the seven-point method when aspect ratio is infinite. Since for a given sweep angle the seven-point solution gives correct values as $A \rightarrow 0$, a function which becomes small as A diminishes is used to bring the corrections at $A = \infty$ down to finite aspect ratios.

The distribution of circulation parameter, $c_l c / c_{av}$, will be corrected in two steps: (1) The taper ratio is altered so as to take into account the error due to the $M = 7$ evaluation of the influence coefficients, and (2) the loading at the root of a swept wing is multiplied by a factor to take into account an error that is largely due to the inability of an $m = 7$ trigonometric loading series to predict the loading at the root.

Two corrective factors will be applied to the lift-curve slope, (1) a factor that takes into account the inability of a seven-point numerical integration to integrate the loading accurately, and (2) a factor that takes into account the added loading at the wing root due to the above second correction.

With the distribution of the circulation parameter $c_l c / c_{av}$ and the lift C_L corrected, the loading coefficient $c_l c / C_L c_{av}$ will be evaluated in terms of the above corrections and values read from the loading charts¹ of reference 1. With the corrected loading at the four span stations known, the loading coefficient at other span stations may be found by using the interpolation formula given as equation (A52) of reference 1. To overcome some shortcomings of this formula, simple additive corrections will be developed. An equation for the spanwise center of pressure, η_{cp} , will also be developed which will take into account the above corrections.

The procedure by which the charts of reference 1 are used to obtain accurate values is summarized in a section following the development. No marked increase of time or labor is involved in obtaining the more accurate results over the ordinary usage of reference 1.

Correction of Distribution of Circulation

Correction at $A = \infty$.— If, with $A = \infty$, M in the Weissinger method is made infinitely large (i.e., the influence coefficients integrated exactly)

¹While the method is developed primarily to apply to loading coefficients given in charts in reference 1, it can also be applied to plan forms beyond the scope of those charts by using values of the a_{vn} coefficients in equation 1 of reference 1 corresponding to the wing with an altered taper ratio.

then the loading due to angle of attack ("additional" loading) is predicted without error for $\eta > 0$. The result for $M = \infty$

$$c_{l_{\alpha}} c_v / c_{av} = (2\pi \cos \Lambda) (c_v / c_{av}) \quad 0 < \eta < 1.0 \quad (1)$$

independent of m . At $\eta = 0$, the $M = \infty$ solution results in

$$\frac{c_{l_{\alpha}} c_v}{c_{av}} = \frac{2\pi \cos \Lambda (c_v / c_{av})}{1 + \sin \Lambda} \quad (2)$$

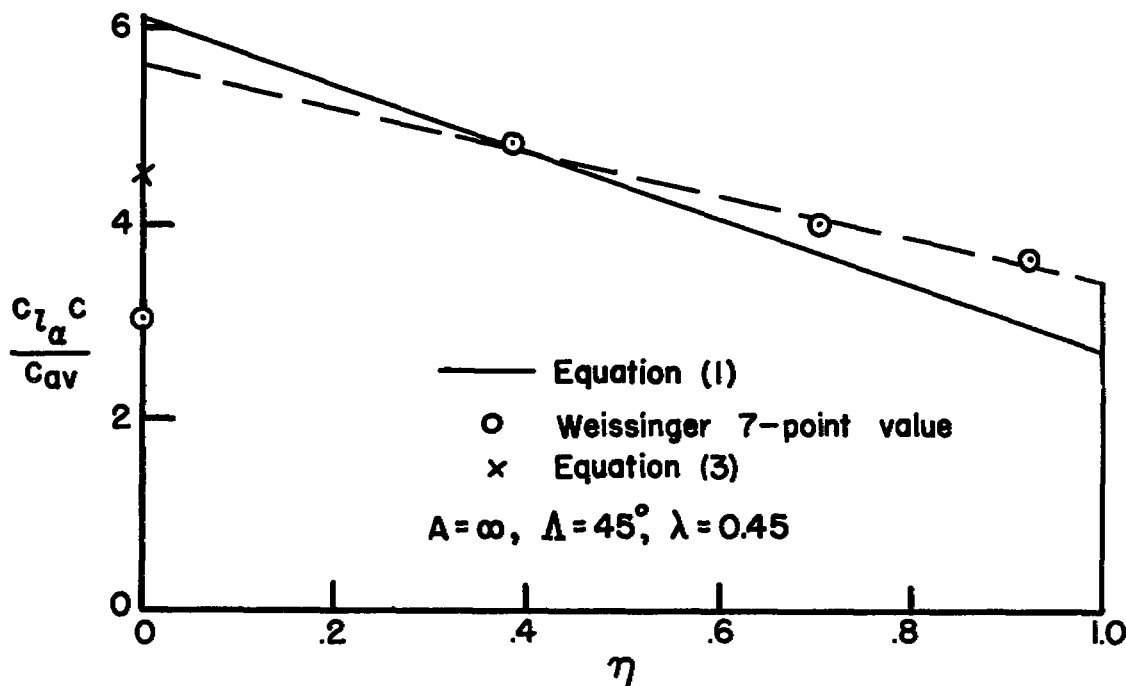
for any finite m . More accurate solutions (refs. 4 and 5) for the loading at the wing root indicate that the values given by equation (2) are substantially low. The root error is attributed largely to the use of a finite m . However, simply taking one half of the value of $\sin \Lambda$ in equation (2) gives an expression that is sufficiently accurate; that is,

$$\frac{c_{l_{\alpha}} c_v}{c_{av}} = \frac{2\pi \cos \Lambda (c_v / c_{av})}{1 + (\sin \Lambda)/2} \quad \eta = 0 \quad (3)$$

The values of loading given by equations (2) and (3) compare with the value given by the $m = M = \infty$ theory of reference 4 and slender wing theory of reference 5 as follows (comparing $c_{l_{\alpha}} / (2\pi \cos \Lambda)$):

Sweep, deg	$\frac{1}{1 + \sin \Lambda}$	$\frac{1}{1 + (\sin \Lambda)/2}$	Accurate values	Reference
0	1.000	1.000	1.000	two-dimensional theory
45	.588	.739	.740	4
90	.500	.667	.637	5

The next step is to find the corresponding Weissinger seven-point results at $\Lambda = \infty$. For $m = M = 7$, the circulation parameter, $c_{l_{\alpha}} c / c_{av}$, can be found by analytical solution of the four downwash equations, as is shown in the appendix. The Weissinger $m = M = 7$ loading and the accurate loading at $\Lambda = \infty$ are compared in the following sketch for $\lambda = 0.45$ and $\Lambda = 45^\circ$. With no spanwise variation of sweep or taper ratio, the accurate loading (eq. (1)) gives for $\eta > 0$ a linear variation of loading related to the taper ratio.



It is seen that at $\eta > 0$ the Weissinger loading values also have an almost linear distribution, but with less slope. The differences between the Weissinger values at $\eta > 0$ and the accurate values will be called the M error. It can be reduced by using a taper ratio (in the Weissinger calculations) lower than the real geometric taper ratio. The ratio of tip value to root value of a line drawn equidistant from the Weissinger values (see sketch) divided into the real taper ratio gives a factor for reducing taper ratio. This factor times the wing taper ratio results in an effective taper ratio, λ_e , for $A = \infty$. By limiting the plan-form characteristics with regard to sweep and taper ratio, it is possible to present the correction in simple form (for $A = \infty$),

$$\lambda_e \approx [1 - 0.004(1 + \lambda)\Lambda^\circ]\lambda \quad (4)$$

for $0.25 < \lambda < 0.75$ and $30^\circ < \Lambda < 80^\circ$.

There remains the error at the wing root. It was shown that with $M = \infty$, the loading at the root can be improved by a correction of the form,

$$\frac{1 + \sin \Lambda}{1 + (\sin \Lambda)/2} = 1 + \frac{\sin \Lambda}{2 + \sin \Lambda} \quad (5)$$

For calculations made with $M = 7$, the M error at $\eta = 0$ is not sufficiently taken into account by the use of the effective taper ratio. It is found that the coefficient, $1.75 - \lambda_e^{1/3}$, applied to the second term

of equation (5) gives values of root loading approximately equal to those given by equation (3). The resulting corrective coefficient of $(c_l c/c_{av})_4$ for $A = \infty$ is

$$\frac{(c_l c/c_{av})_4 + \Delta(c_l c/c_{av})_4}{(c_l c/c_{av})_4} = 1 + \sigma_\infty \quad (6)$$

where

$$\sigma_\infty = \frac{\sin \Lambda (1.75 - \lambda_e^{1/3})}{2 + \sin \Lambda} \quad (7)$$

Thus, if the loading for an $m = M = 7$ Weissinger solution for $A = \infty$ is obtained using the taper ratio given by equation (4) and the consequent loading at midwing is multiplied by equation (6), then the wing loading at the four span stations is accurate within a few percent for the stated range of values of sweep and taper ratio. This compares with errors of up to 35 percent for the noncorrected $m = M = 7$ method at $A = \infty$.

Corrections for arbitrary aspect ratio.—The magnitude of the corrections should diminish with decreasing aspect ratio since the need for corrections vanishes as $A \rightarrow 0$ for finite sweep. A function of the form,

$\frac{1}{1 + (k/A)^2}$ was found to be suitable for multiplying the corrective terms

of equations (4) and (6). A value of k for each of the corrections can be determined so that the corrected loading values at all values of η are within ± 1 percent of those obtained by the Multhopp 23-point method for an $A = 8$, $\Lambda = 45^\circ$, and $\lambda = 0.45$ wing reported in reference 3. With the values of k determined, the effective taper ratio of the wings of arbitrary aspect ratio becomes

$$\lambda_e = \left[1 - \frac{0.004(1 + \lambda)\Lambda^\circ}{1 + (7/A)^2} \right] \lambda \quad (8)$$

and the correction at the root, σ , becomes

$$\sigma = \frac{(1.75 - \lambda_e^{1/3}) \sin \Lambda}{[1 + (24/A)^2](2 + \sin \Lambda)} \quad (9)$$

Total lift

Since the span-loading curves are not well approximated by a four-term trigonometric series, an $m = 7$ numerical integration of spanwise loading does not give sufficiently accurate results for swept wings of high aspect ratio. An approximate correction for the integration error

can be found. Also, the added loading at the root of a sweptback wing adds to the total lift and must be taken into account.

Correction for numerical integration.- The correction can be estimated by first finding the error of a seven-point integration of an analytical loading whose integrated lift is known and whose form is reasonably typical of high-aspect-ratio wings. The first approximation to such a loading distribution is the distribution at $A = \infty$. From equation (1), for $\eta > 0$ the loading coefficient, K_n , (see list of symbols) reduces to

$$K_n = \left(\frac{c}{c_{av}} \right)_n = \frac{2}{1 + \lambda} [1 - \eta(1 - \lambda)] \quad (10a)$$

for straight-tapered wings. From equation (3), for $\eta = 0$

$$K_4 = \frac{(c/c_{av})_4}{1 + (\sin \Lambda)/2} = \frac{2}{(1 + \lambda)[1 + (\sin \Lambda)/2]} \quad (10b)$$

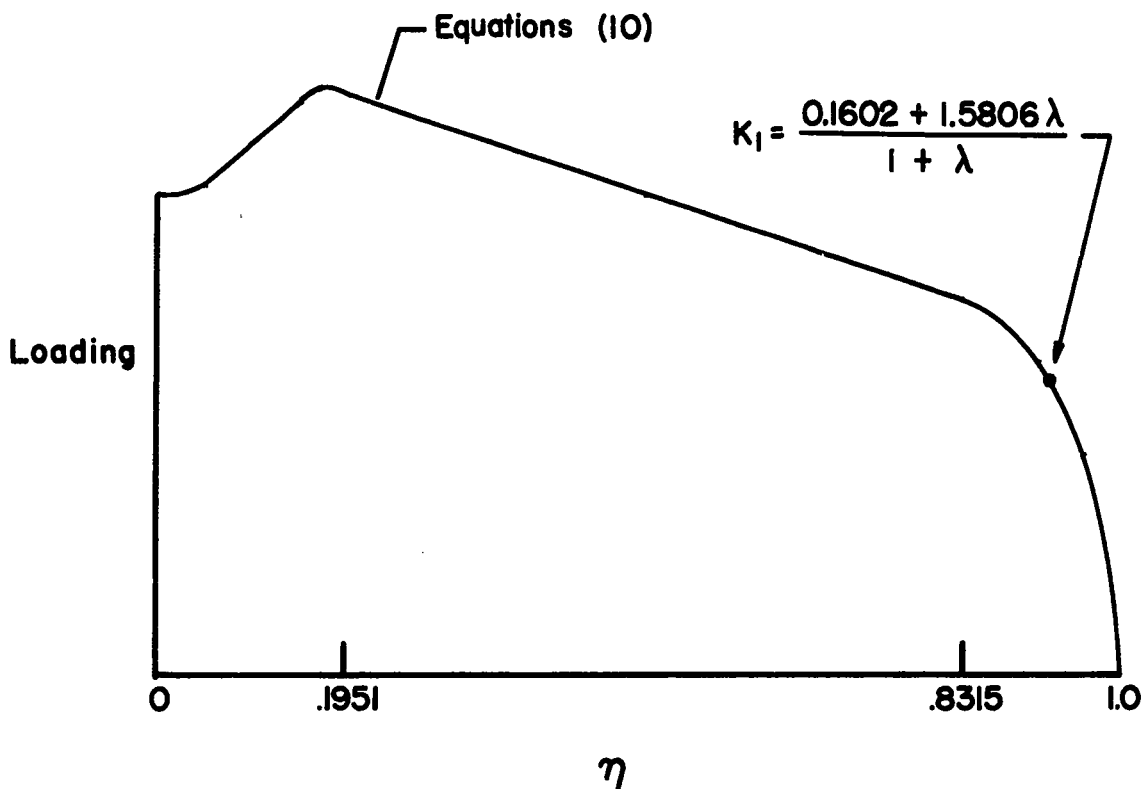
also for straight-tapered wings. Such a loading distribution has an infinite loading gradient at the wing tip and at the wing root; however, the aspect ratio would have to be extremely large to approach this condition. Here, in order not to demand too much from a seven-point integration, the wing tip loading and the loading at the wing root will be rounded off to approximate the behavior of a wing of $A \approx 20$. At the wing tip, from $\eta = 0.8315$ to 1.0000, the loading is assumed of the form

$$K = a_1 \sin \phi + a_3 \sin 3\phi \quad (11)$$

where a_1 and a_3 are determined by the requirement that the loading and loading slope equal that given by equation (10a) at $\eta = 0.8315$. At the wing root, from $\eta = 0$ to 0.1951, the loading is assumed of the form

$$K = b_1 \sin \phi + b_3 \sin 3\phi + b_5 \sin 5\phi \quad (12)$$

where b_1 , b_3 , and b_5 are determined by the requirements that the loading at $\eta = 0$ and 0.1951 and that the slope of the loading at $\eta = 0.1951$ equal values given by equation (10b). The final distribution of loading with the rounding off at the tip and root is shown in the following sketch:



Since the loading is known analytically, the area beneath the curve can be determined exactly. The area is

$$\frac{2.0028 + 1.8692\lambda + 0.8547 \sin \Lambda + 0.9346\lambda \sin \Lambda}{(1 + \lambda)(2 + \sin \Lambda)}$$

It is convenient to raise the loading values so that the curve has unit area by dividing by the above expression. The seven-point integration formula of reference 1 can now be applied and the errors of the formula can be determined. The seven-point integration formula is (from ref. 1)

$$(C_{L\alpha})_7 = \frac{\pi}{16} \left[0.7654 \left(\frac{c_{l\alpha}^c}{c_{av}} \right)_1 + 1.4142 \left(\frac{c_{l\alpha}^c}{c_{av}} \right)_2 + 1.8474 \left(\frac{c_{l\alpha}^c}{c_{av}} \right)_3 + \left(\frac{c_{l\alpha}^c}{c_{av}} \right)_4 \right] \quad (13)$$

The ratio of the seven-point value to the exact value of $C_{L\alpha}$ may be written

$$\frac{(C_{L\alpha})_7}{(C_{L\alpha})_{\text{exact}}} = \frac{\pi}{16} (0.7654K_1 + 1.4142K_2 + 1.8474K_3 + K_4) \quad (14)$$

where the K 's are the previously determined loading values with unit area. Equation (14) does not yield unit area. The discrepancy will be called the integration error, γ , or

$$C_{L\alpha} = (1 + \gamma)(C_{L\alpha})_7 \quad (15)$$

The quantity, γ , is virtually independent of taper ratio in the range $0.25 < \lambda < 0.75$ and can be given as simply

$$\gamma = \frac{\sin \Lambda}{20} \quad (16)$$

While the above value is probably more representative of integration error at $A \sim 20$, it is convenient to take this value for $A = \infty$. Applying the aspect-ratio function, $\frac{1}{1 + (k/A)^2}$, and setting k to yield the Multhopp results for the $A = 8$ wing mentioned previously, yields the following expression for γ at arbitrary aspect ratios

$$\gamma = \frac{\sin \Lambda}{20 \left[1 + \left(\frac{11.7}{A} \right)^2 \right]} \quad (17)$$

Correction for added root loading.— The product of $c_l c / c_{av}$ and σ gives the increase of root section loading due to the root correction. The increment of $C_{L\alpha}$ due to this added loading is, from equation (14),

$$\Delta C_{L\alpha} = \frac{\pi \sigma K_4 (C_{L\alpha})_{\lambda_e}}{16} \quad (18)$$

For the range of plan forms under consideration (positive sweep and conventional taper), K_4 may be taken as slightly larger than unity. Thus,

$$\Delta C_{L\alpha} \simeq \frac{\sigma}{5} (C_{L\alpha})_{\lambda_e} \quad (19)$$

The quantity $(C_{L\alpha})_{\lambda_e}$ is the seven-point value for a wing with the effective taper ratio rather than the geometric taper ratio (read from the $C_{L\alpha}$ charts of ref. 1). Thus,

$$(C_{L\alpha})_7 = \left(1 + \frac{\sigma}{5}\right)(C_{L\alpha})_{\lambda_e} \quad (20)$$

Inserting equation (20) into equation (15) and dropping the second-order term $\frac{\gamma\sigma}{5}$, yields the corrected total lift as

$$C_{L\alpha} = \left(1 + \gamma + \frac{\sigma}{5}\right)(C_{L\alpha})_{\lambda_e} \quad (21)$$

where $(C_{L\alpha})_{\lambda_e}$ may be read from figure 4 of reference 1, γ is given by equation (17), and σ is given by equation (9).

Corrected Loading Coefficient and Interpolation

Corrected loading coefficient.— The loading coefficient, $K_n = (c_l c / C_{L\alpha})_n$ determined, say, from the charts of reference 1 by using the effective taper ratio (eq. (8)) and the root correction (eq. (9)) will need a final correction since the total lift coefficient, $C_{L\alpha}$, has changed (eq. (21)). The K_n 's become

$$\left. \begin{aligned} K_n &= \frac{(K_n)_7 \lambda_e}{1 + \gamma + (\sigma/5)} \\ K_4 &= \frac{(1 + \sigma)(K_4)_7 \lambda_e}{1 + \gamma + (\sigma/5)} \end{aligned} \right\} \quad (22)$$

Interpolation.— The seven-point interpolation, equation (A51) of reference 1, of loading at span stations between the four known loading values, gives the loading distribution which the seven-point numerical integration formula integrates when obtaining total lift. Thus the error in interpolating is related to the error when integrating. The values of K_n for the preceding rounded-off loading assumed for $A = \infty$ can be interpolated by equation (A52) of reference 1. The differences of the interpolated from the accurate loading were found to be nearly directly proportional to γ_∞ (given in eq. (16)). The effect of taper ratio is nil and is omitted. Thus the increments of loading to be added to interpolated results at $\eta = 0.1951$, 0.5556 , and 0.8315 , were found to be

$$\left. \begin{aligned} \Delta K_{7/2} &= 5.15\gamma_{\infty} \\ \Delta K_{5/2} &= -1.55\gamma_{\infty} \\ \Delta K_{3/2} &= 1.03\gamma_{\infty} \end{aligned} \right\} \quad (23)$$

respectively. No reliable value of $\Delta K_{1/2}$ could be found and $\Delta K_{1/2}$ is taken as zero.

If the interpolation error is assumed to decrease with aspect ratio in the same manner as the lift integration error, γ , then at finite aspect ratios

$$\left. \begin{aligned} \Delta K_{7/2} &= 5.15\gamma \\ \Delta K_{5/2} &= -1.55\gamma \\ \Delta K_{3/2} &= 1.03\gamma \\ \Delta K_{1/2} &\sim 0 \end{aligned} \right\} \quad (24)$$

which gives the correction to be added to interpolated loadings at $\eta = 0.1951, 0.5556, 0.8315$, and 0.9808 , respectively.

Spanwise Center of Pressure

The spanwise center of pressure is given by

$$\eta_{cp} = \frac{\int_{\eta=0}^{1.0} (c_l c / c_{av}) \eta \, d\eta}{\int_{\eta=0}^{1.0} (c_l c / c_{av}) \, d\eta} \quad (25)$$

Letting $\eta = \cos \phi$ and multiplying the numerator and the denominator by $c_{av}/2b$ gives

$$\eta_{cp} = \frac{\int_0^{\pi/2} G(\phi) \sin \phi \cos \phi \, d\phi}{\int_0^{\pi/2} G(\phi) \sin \phi \, d\phi} \quad (26)$$

By use of the loading series given by equation (A17), reference 1, the integrals can be evaluated. Taking $m = 15$, and using the seven-point interpolated values of loading corrected by equation (24), we obtain for the spanwise center of pressure

$$\eta_{cp} = \frac{0.352K_1 + 0.503K_2 + 0.344K_3 + 0.041K_4 + 0.364\gamma}{0.383K_1 + 0.707K_2 + 0.924K_3 + 0.500K_4 + 2.155\gamma} \quad (27)$$

where the K values are for unit area.

SUMMARY OF PROCEDURE

For wings with taper ratios, λ , between 0.25 and 0.75 and whose quarter-chord lines are swept back between 30° and 80° ,² the following parameters are evaluated

$$\lambda_e = \left[1 - \frac{0.004(1 + \lambda)\Lambda^0}{1 + (7/\Lambda)^2} \right] \lambda$$

$$\gamma = \frac{\sin \Lambda}{20[1 + (11.7/\Lambda)^2]}$$

$$\sigma = \frac{(1.75 - \lambda_e^{1/3}) \sin \Lambda}{[1 + (24/\Lambda)^2](2 + \sin \Lambda)}$$

From either the loading charts of reference 1 or simultaneous solution of equation (1) of reference 1, the loading coefficients K_{n7} are obtained for the wing parameters A , Λ , and λ_e . The K_{n7} values are then multiplied by correction factors as follows:

$$K_n = \frac{K_{n7}}{1 + \gamma + (\sigma/5)} \quad \text{for } \eta = 0.9239, 0.7071, \text{ and } 0.3827$$

$$K_4 = \frac{(1 + \sigma)K_{47}}{1 + \gamma + (\sigma/5)} \quad \text{for } \eta = 0$$

²Such large angles of sweep might be the result of applying the Prandtl-Glauert transformation to take account of compressibility; that is, an angle of sweep, Λ_β , is used such that

$$\tan \Lambda_\beta = \left(\frac{1}{\sqrt{1 - M_o^2}} \right) \tan \Lambda$$

and

$$C_{L\alpha} = [(1 + \gamma + (\sigma/5)](C_{L\alpha})_7$$

With the improved loading at the four span stations known, the loading coefficient at other span stations may be found by using the interpolation formula given as equation (A52) of reference 1. However, to these interpolated values the following corrections should be added:

$$\Delta K_{7/2} = 5.15\gamma, \quad \eta = 0.1951$$

$$\Delta K_{5/2} = -1.55\gamma, \quad \eta = 0.5556$$

$$\Delta K_{3/2} = 1.03\gamma, \quad \eta = 0.8315$$

$$\Delta K_{1/2} \sim 0, \quad \eta = 0.9808$$

The spanwise center of pressure, η_{cp} , is found as

$$\eta_{cp} = \frac{0.352K_1 + 0.503K_2 + 0.344K_3 + 0.041K_4 + 0.364\gamma}{0.383K_1 + 0.707K_2 + 0.924K_3 + 0.500K_4 + 2.155\gamma}$$

RESULTS AND DISCUSSION

Comparison of Modified Seven-Point Results With Other Theoretical Results

In figure 2, comparisons are presented for the following plan forms:

A	Sweep, deg	Taper	Method
10	40	0.40	Falkner 19-point
8	45	.45	Multhopp 23-point
7	35	.50	Weissinger 15-point
2.64	45	.389	Multhopp 15-point
6	45	0	Multhopp 15-point

For a discussion of the methods, see reference 3.

In figures 2(a), (b), (c), and (d), it is seen that the new results are much more accurate than the original Weissinger seven-point results which are also shown. The new span loadings for these wings are within about ± 1 percent of the results of the more lengthy methods. In contrast, the maximum errors of the original Weissinger loadings range from approximately 2 to 8 percent for wings of aspect ratios of 3 to 10.

As has been pointed out, the corrections are not valid for $\lambda < 0.25$. In figure 2(e), the "corrections" at $\lambda = 0$ are seen to be detrimental to the accuracy of the span loading.

Comparison of Modified Seven-point Results with Experiment

In figure 3, the new results and the original Weissinger results are compared with high Reynolds number experimental results for the following wings:

A	Sweep, deg	Taper	Source	R
10	40	0.40	unpublished	8×10^6
8	45	.45	ref. 3	4×10^6
6	45	.29	unpublished	5.8×10^6
6	45	.50	ref. 6	8×10^6

The first two wings have truly high aspect ratios and it is seen that the new span loadings and lift-curve slopes are in good agreement with the experimental results on these wings.³

The third and fourth wings were in combination with fuselages. The influence of the fuselage of the fourth wing is seen in the magnitude of the experimental loading at $\eta = 0.17$. Outboard of $\eta = 0.3$ where the influence of the fuselage is fairly small, the new results are appreciably closer to experiment than are the original Weissinger results. Thus, these two comparisons also tend to confirm the new results.

To obtain the simplicity of the present corrections, it was necessary to limit the taper ratio to $0.25 < \lambda < 0.75$ and the sweep angle to $30^\circ < \Lambda < 80^\circ$. However, it is interesting to note in figure 2(e) that the lift-curve slope for $\lambda = 0$ is improved by the correction. To determine whether such improvement is possible for untapered wings, some experimental and corrected lift-curve slopes for $\Lambda = 60^\circ$ have been compared in figure 4. It is seen that for even these extreme plan forms, the $C_{L\alpha}$ correction improves the original Weissinger values and results in reasonable agreement with experiment. Thus, it appears that in the case of $C_{L\alpha}$ the correction is beneficial at all taper ratios.

³It is true that the Falkner 19-point and Multhopp 23-point methods also agree with these experimental data but at the cost of much more time and labor.

CONCLUSIONS

The general accord of the new results with results believed to be accurate indicates that the corrections yield very acceptable answers. Simplicity in the corrections has been attained.

Ames Aeronautical Laboratory
National Advisory Committee for Aeronautics
Moffett Field, Calif., Apr. 26, 1955

APPENDIX

The solution for spanwise loading by the Weissinger method for $A = \infty$, is readily obtained from reference 7. Equation (B2) of reference 7 gives values of A_{vn} for high aspect ratio, in terms of Λ and the parameter,

$$H_v \equiv d_v(b/c_v)$$

where d_v is simply a scale factor and is listed below,

v	d_v
1	0.061
2	.234
3	.381
4	.320

As $A \rightarrow \infty$, only the term that contains H_v becomes significant. Inserting A_{vn} for $A = \infty$, we can write equation (1) of reference 6 as follows:

$$\frac{c_v}{c_{av}} \alpha_v = \sum_{n=1}^4 \left(\frac{s_{vn}}{\cos \Lambda} + t_{vn} \tan \Lambda \right) \left(\frac{c_l c}{c_{av}} \right)_n, \quad v = 1, 2, 3, \text{ and } 4 \quad (A1)$$

where s_{vn} and t_{vn} are $d_v/2$ times the respective numbers in the coefficient of H_v in equation (B2) of reference 7. The s_{vn} and t_{vn} are listed as follows:

$v \backslash n$	s_{vn}				t_{vn}			
	1	2	3	4	1	2	3	4
1	0.1192	0.0271	-0.0074	0.0052	0.0442	0.0479	-0.0130	0.0052
2	.0271	.1114	.0325	-.0156	-.1155	.0313	.0477	-.0156
3	-.0078	.0323	.1036	.0594	.0755	-.1155	.0442	.0594
4	.0026	-.0078	.0297	.1114	-.0339	.0442	-.0817	.1114

The simultaneous solution of the four equations given by equation (A1) results in the evaluation of loading at four spanwise stations.

$$\left. \begin{aligned}
 \left(\frac{c_l c}{c_{av}} \right)_1 &= \frac{\cos \Lambda}{(1+\sin \Lambda)^4} \left[9.28(1+\sin \Lambda)^3 \frac{c_1}{c_{av}} \alpha_1 + (-3.05+15.51\sin \Lambda) \right. \\
 &\quad (1+\sin \Lambda)^2 \frac{c_2}{c_{av}} \alpha_2 + (2.23-20.18\sin \Lambda+14.71\sin^2 \Lambda)(1+\sin \Lambda) \frac{c_3}{c_{av}} \alpha_3 + \\
 &\quad \left. (-1.02+11.49\sin \Lambda-17.13\sin^2 \Lambda+7.45\sin^3 \Lambda) \frac{c_4}{c_{av}} \alpha_4 \right] \\
 \left(\frac{c_l c}{c_{av}} \right)_2 &= \frac{\cos \Lambda}{(1+\sin \Lambda)^4} \left[-3.05(1+\sin \Lambda)^3 \frac{c_1}{c_{av}} \alpha_1 + (11.52+5.42\sin \Lambda) \right. \\
 &\quad (1+\sin \Lambda)^2 \frac{c_2}{c_{av}} \alpha_2 + (-5.09+18.93\sin \Lambda+11.83 \sin^2 \Lambda)(1+\sin \Lambda) \frac{c_3}{c_{av}} \alpha_3 + \\
 &\quad \left. (2.24-12.93\sin \Lambda+2.62\sin^2 \Lambda+5.60\sin^3 \Lambda) \frac{c_4}{c_{av}} \alpha_4 \right] \\
 \left(\frac{c_l c}{c_{av}} \right)_3 &= \frac{\cos \Lambda}{(1+\sin \Lambda)^4} \left[2.23(1+\sin \Lambda)^3 \frac{c_1}{c_{av}} \alpha_1 + (-5.10-0.63\sin \Lambda) \right. \\
 &\quad (1+\sin \Lambda)^2 \frac{c_2}{c_{av}} \alpha_2 + (13.74+12.83\sin \Lambda+8.03\sin^2 \Lambda)(1+\sin \Lambda) \frac{c_3}{c_{av}} \alpha_3 + \\
 &\quad \left. (-4.08+8.85\sin \Lambda+10.80\sin^2 \Lambda+6.81\sin^3 \Lambda) \frac{c_4}{c_{av}} \alpha_4 \right] \\
 \left(\frac{c_l c}{c_{av}} \right)_4 &= \frac{\cos \Lambda}{(1+\sin \Lambda)^4} \left[-2.05(1+\sin \Lambda)^3 \frac{c_1}{c_{av}} \alpha_1 + (4.47+0.38\sin \Lambda) \right. \\
 &\quad (1+\sin \Lambda)^2 \frac{c_2}{c_{av}} \alpha_2 + (-8.14-3.25\sin \Lambda-3.30\sin^2 \Lambda)(1+\sin \Lambda) \frac{c_3}{c_{av}} \alpha_3 + \\
 &\quad \left. (11.51+19.89\sin \Lambda+22.35\sin^2 \Lambda+5.79\sin^3 \Lambda) \frac{c_4}{c_{av}} \alpha_4 \right]
 \end{aligned} \right\} (A2)$$

For straight-tapered wings and for additional loading ($\alpha_v = \alpha$), equation (A2) reduces to

$$\begin{aligned}
 \left(\frac{c_{l\alpha}^c}{c_{av}} \right)_1 &= \frac{\cos \Lambda}{(1+\lambda)(1+\sin \Lambda)^4} [0.33 + 10.58 \sin \Lambda - 20.39 \sin^2 \Lambda + \\
 &\quad 43.55 \sin^3 \Lambda + (14.54 + 36.46 \sin \Lambda + 50.34 \sin^2 \Lambda)(1+\sin \Lambda)\lambda] \\
 \left(\frac{c_{l\alpha}^c}{c_{av}} \right)_2 &= \frac{\cos \Lambda}{(1+\lambda)(1+\sin \Lambda)^4} [4.47 + 6.49 \sin \Lambda + 51.33 \sin^2 \Lambda + 28.52 \sin^3 \Lambda + \\
 &\quad (6.86 + 27.39 \sin \Lambda + 11.19 \sin^2 \Lambda)(1+\sin \Lambda)\lambda] \\
 \left(\frac{c_{l\alpha}^c}{c_{av}} \right)_3 &= \frac{\cos \Lambda}{(1+\lambda)(1+\sin \Lambda)^4} [6.16 + 45.17 \sin \Lambda + 44.65 \sin^2 \Lambda + \\
 &\quad 23.50 \sin^3 \Lambda + (7.44 + 9.98 \sin \Lambda + 9.38 \sin^2 \Lambda)(1+\sin \Lambda)\lambda] \\
 \left(\frac{c_{l\alpha}^c}{c_{av}} \right)_4 &= \frac{\cos \Lambda}{(1+\lambda)(1+\sin \Lambda)^4} [15.29 + 30.25 \sin \Lambda + 38.74 \sin^2 \Lambda + \\
 &\quad 7.41 \sin^3 \Lambda - (3.68 + 3.20 \sin \Lambda + 5.78 \sin^2 \Lambda)(1+\sin \Lambda)\lambda]
 \end{aligned}
 \tag{A3}$$

REFERENCES

1. DeYoung, John, and Harper, Charles W.: Theoretical Symmetric Span Loading at Subsonic Speeds for Wings Having Arbitrary Plan Form. NACA Rep. 921, 1948.
2. Garner, H. C.: Swept-Wing Loading. A Critical Comparison of Four Subsonic Vortex Sheet Theories. CP 102, British A.R.C., 1952.
3. Schneider, William C.: A Comparison of the Spanwise Loading Calculated by Various Methods with Experimental Loadings Obtained on a 45° Swept-Back Wing of Aspect Ratio 8 at a Reynolds Number of 4.0×10^6 . NACA RM L51G30, 1952.
4. Multhopp, Hans: Methods for Calculating the Lift Distribution of Wings (Subsonic Lifting Surface Theory). Rep. Aero. 2353, R.A.E. British, Jan. 1950.
5. Jones, Robert T.: Properties of Low-Aspect-Ratio Pointed Wings at Speeds Below and Above the Speed of Sound. NACA Rep. 835, 1946.
6. Hunton, Lynn W.: Effects of Finite Span on the Section Characteristics of Two 45° Sweptback Wings of Aspect Ratio 6. NACA TN 3008, 1953.
7. DeYoung, John: Theoretical Symmetric Span Loading Due to Flap Deflection for Wings of Arbitrary Plan Form at Subsonic Speeds. NACA Rep. 1071, 1952.
8. Goodman, Alex, and Brewer, Jack D.: Investigation at Low Speeds of the Effect of Aspect Ratio and Sweep on Static and Yawing Stability Derivatives of Untapered Wings. NACA TN 1669, 1948.

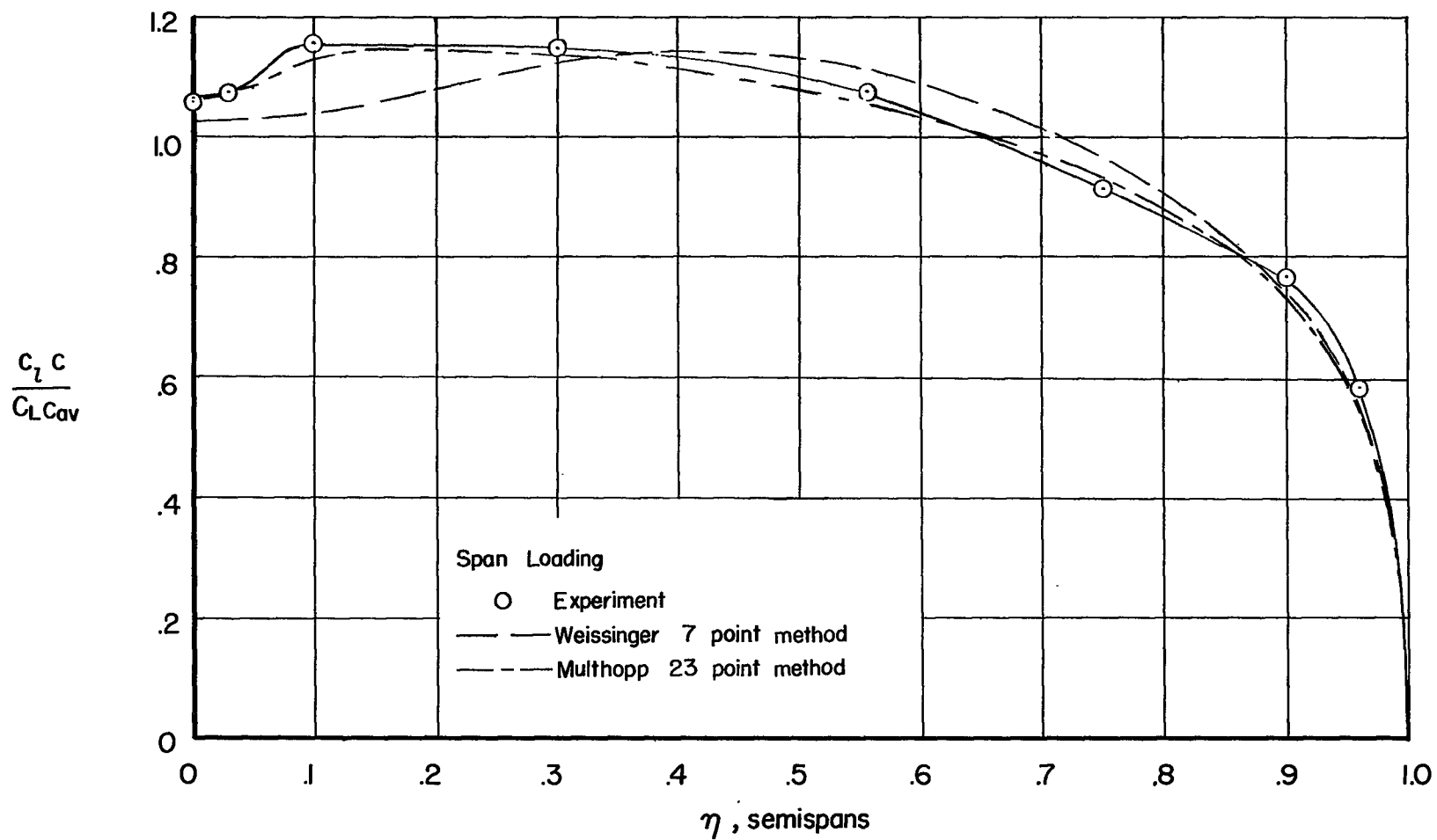
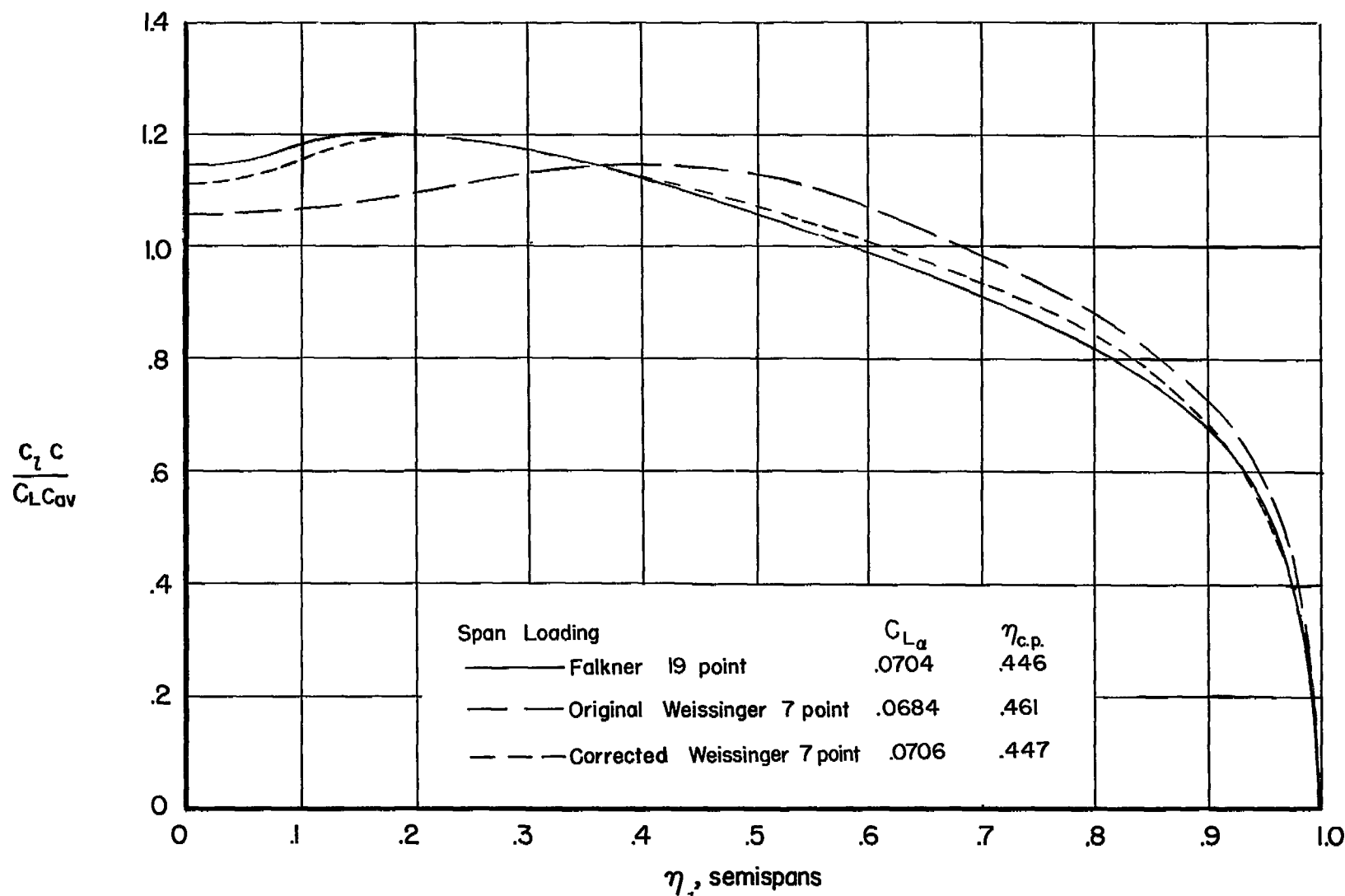
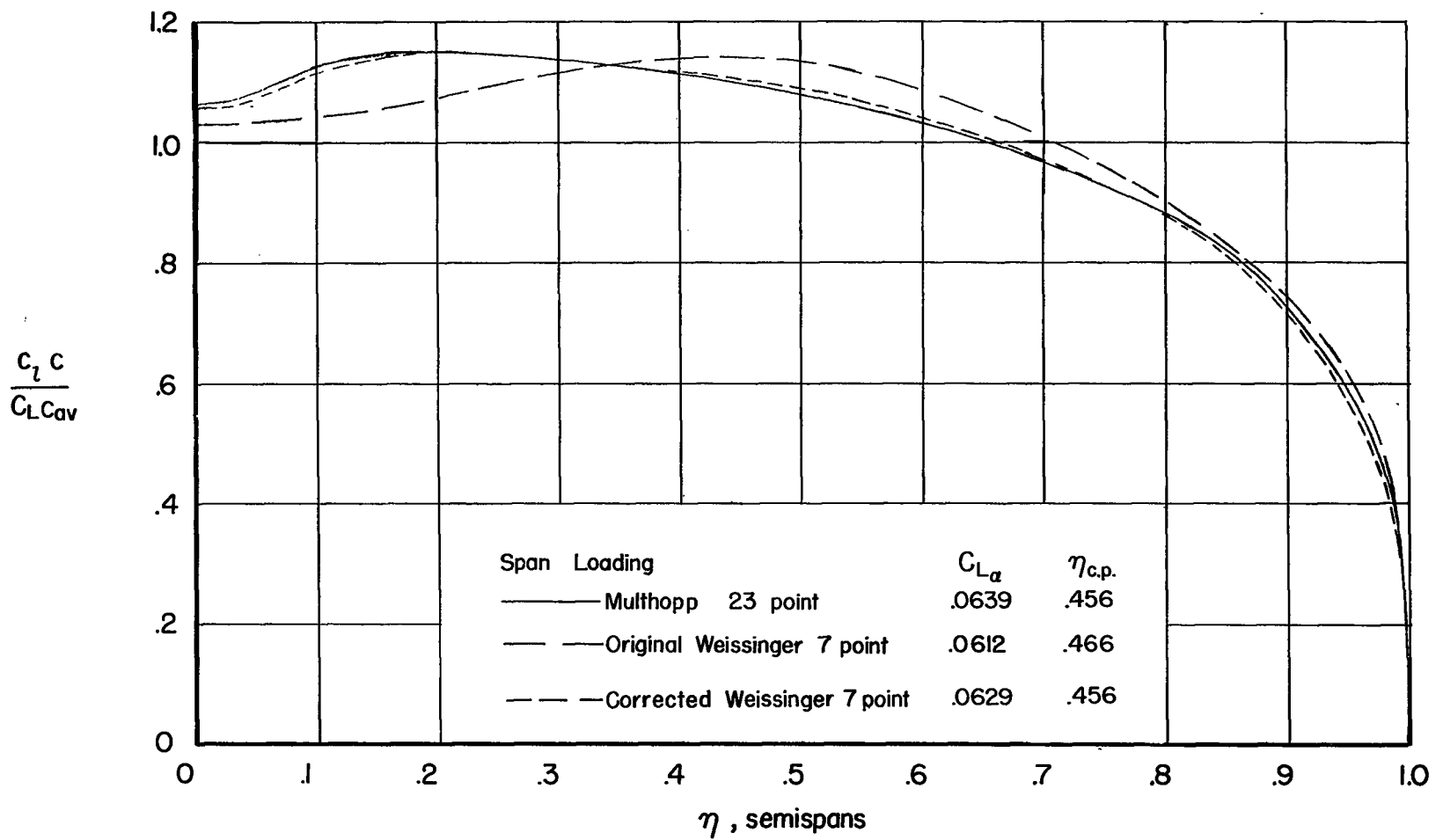


Figure 1.- Comparison of Weissinger 7-point span loading with experiment for $A = 8$, $\Lambda = 45^\circ$, and $\lambda = 0.45$.



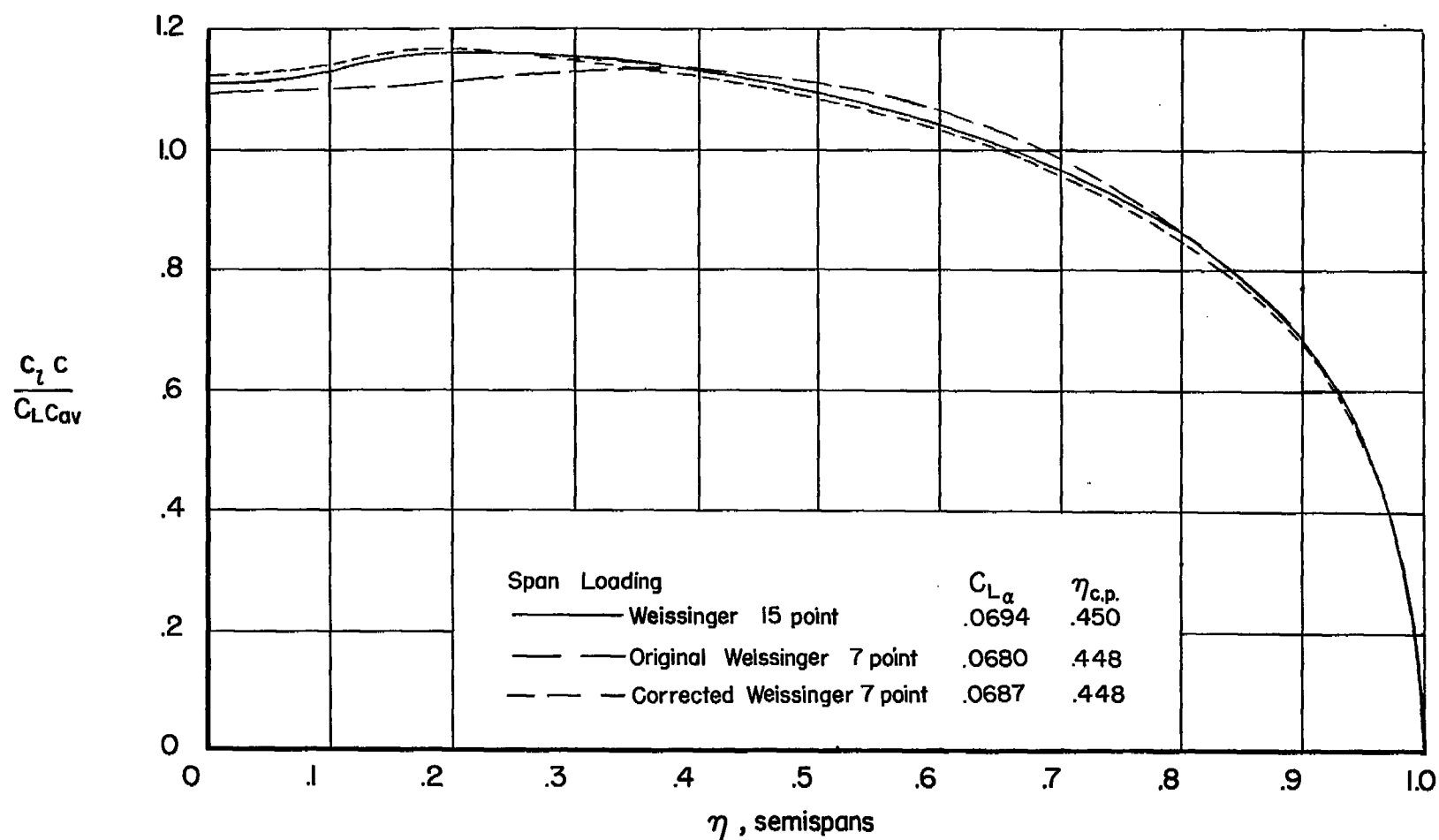
(a) $A = 10$, $\Lambda = 40^\circ$, $\lambda = 0.4$.

Figure 2.- Comparison of 7-point results with other theoretical results.



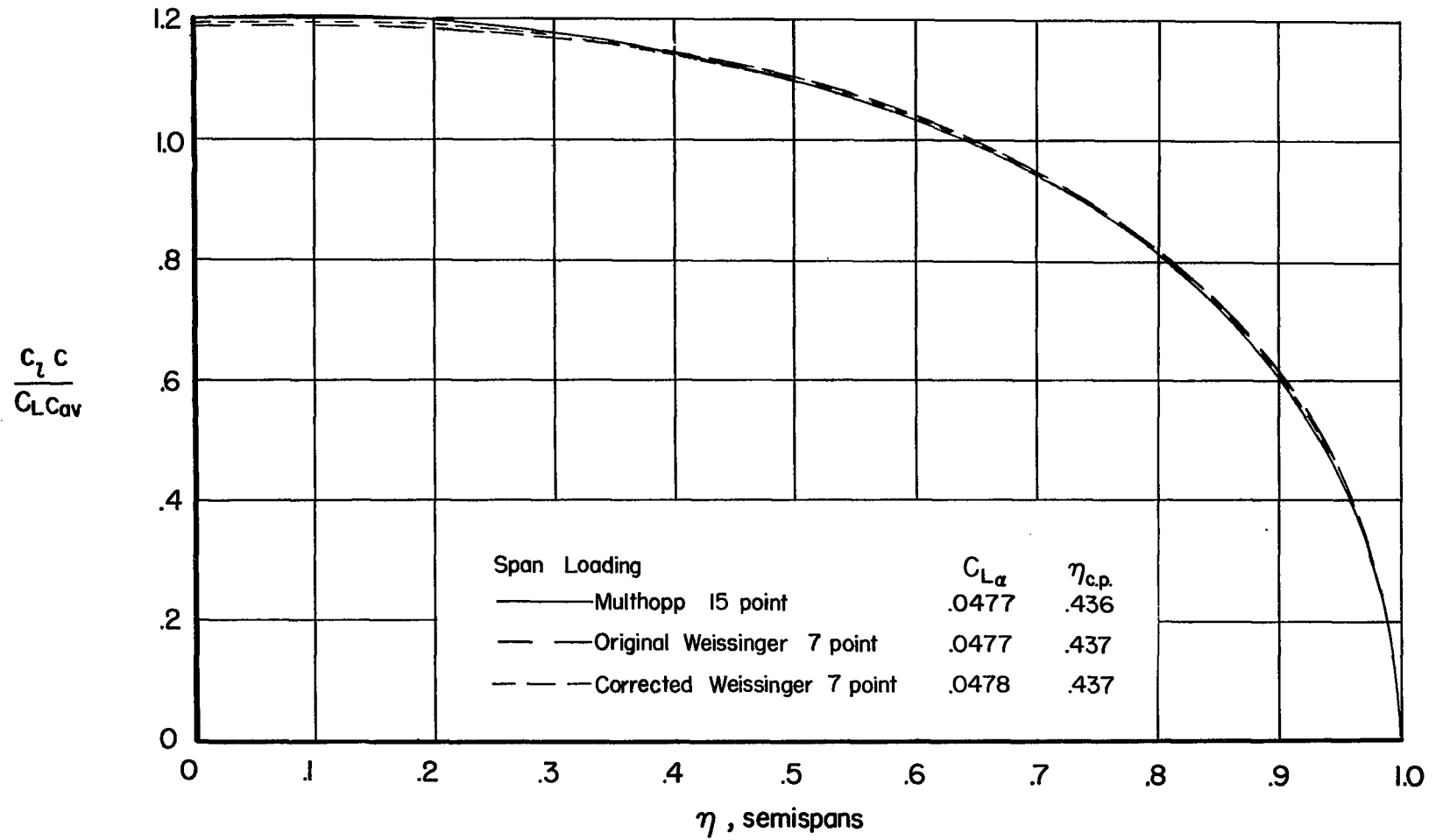
(b) $A = 8$, $\Lambda = 45^\circ$, $\lambda = 0.45$.

Figure 2.- Continued.



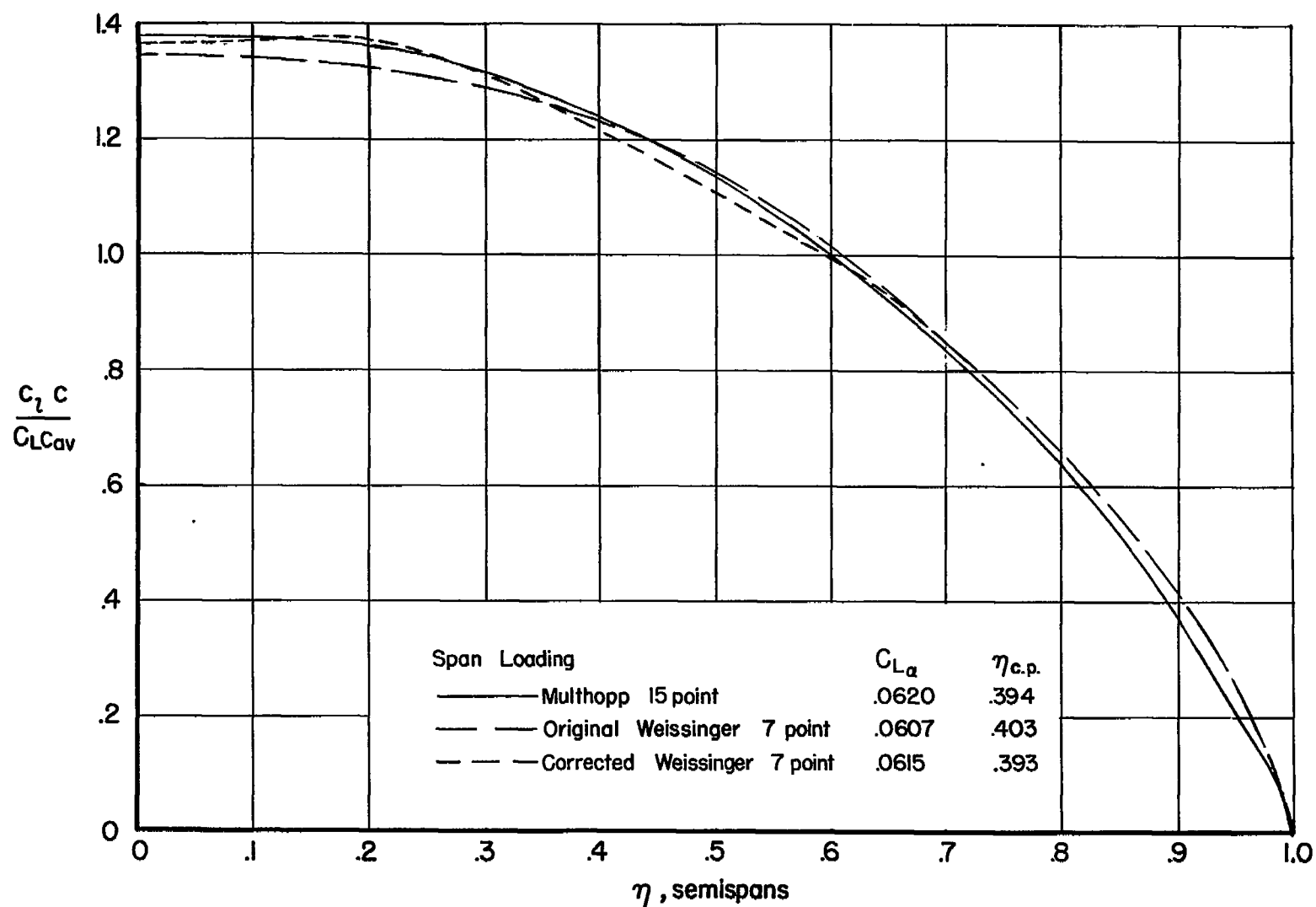
(c) $A = 7$, $\Lambda = 35^\circ$, $\lambda = 0.5$.

Figure 2.- Continued.



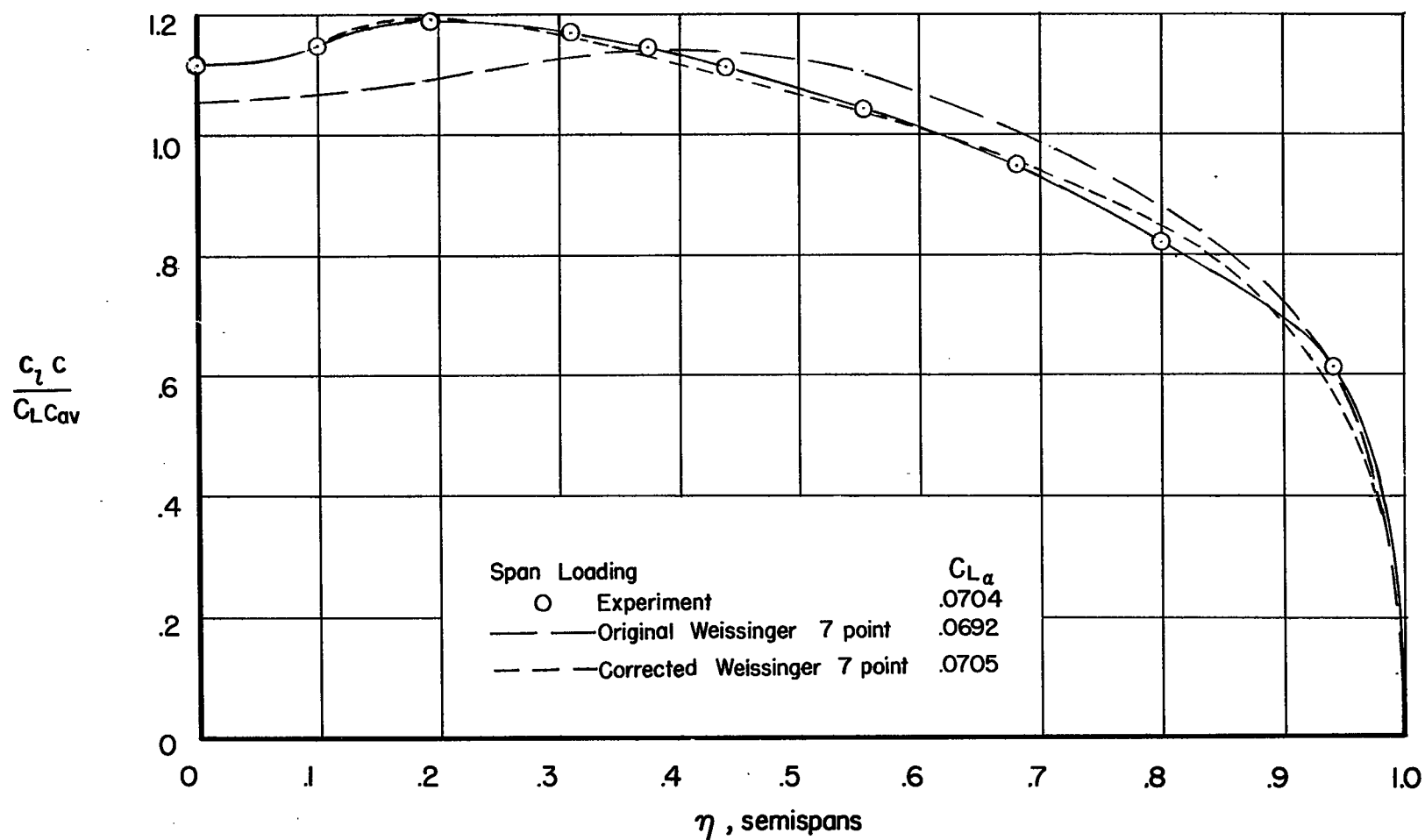
(d) $A = 2.64$, $\Lambda = 45^\circ$, $\lambda = 0.389$.

Figure 2.- Continued.



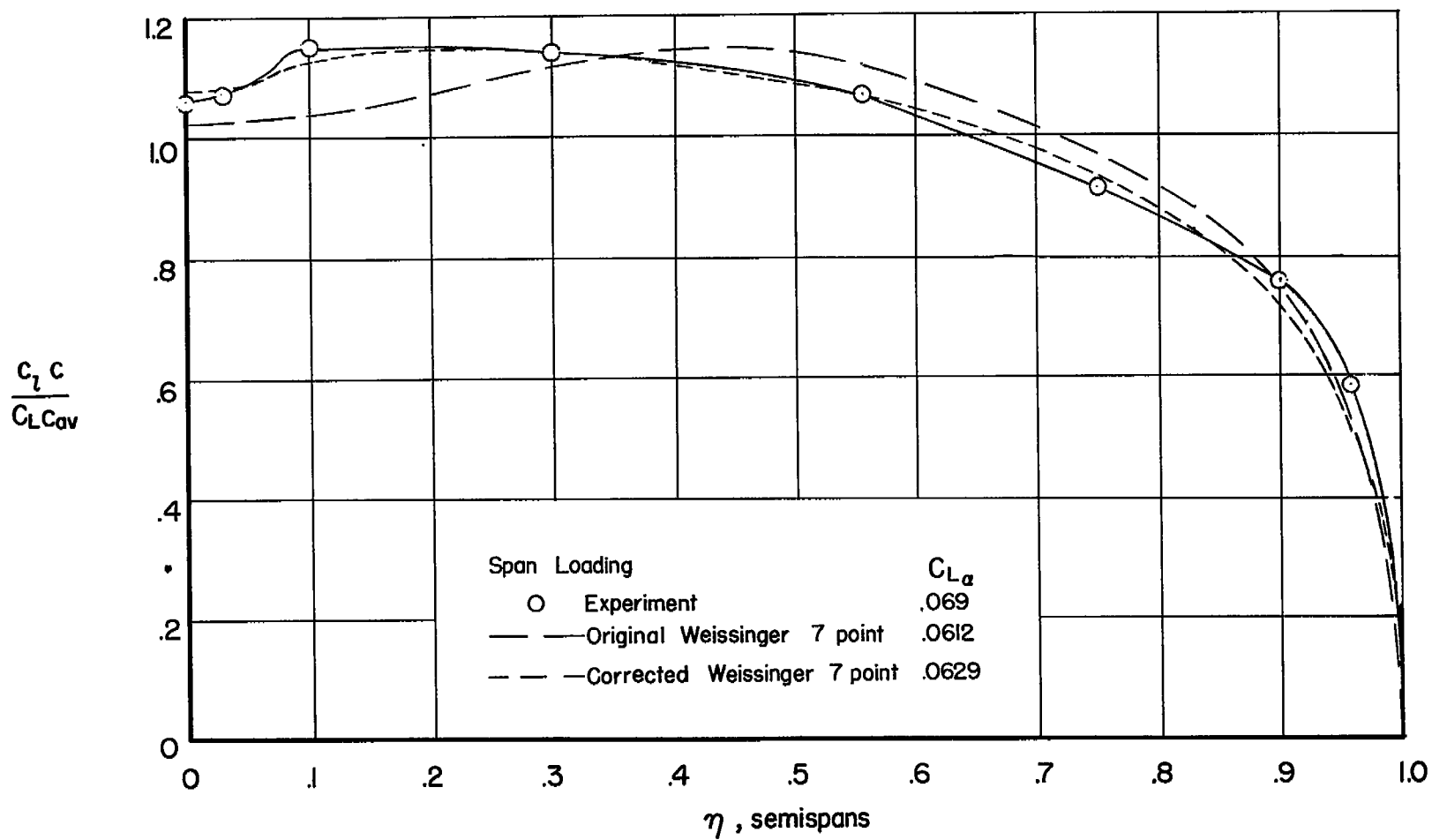
(e) $A = 6$, $\Lambda = 45^\circ$, $\lambda = 0$.

Figure 2.- Concluded.



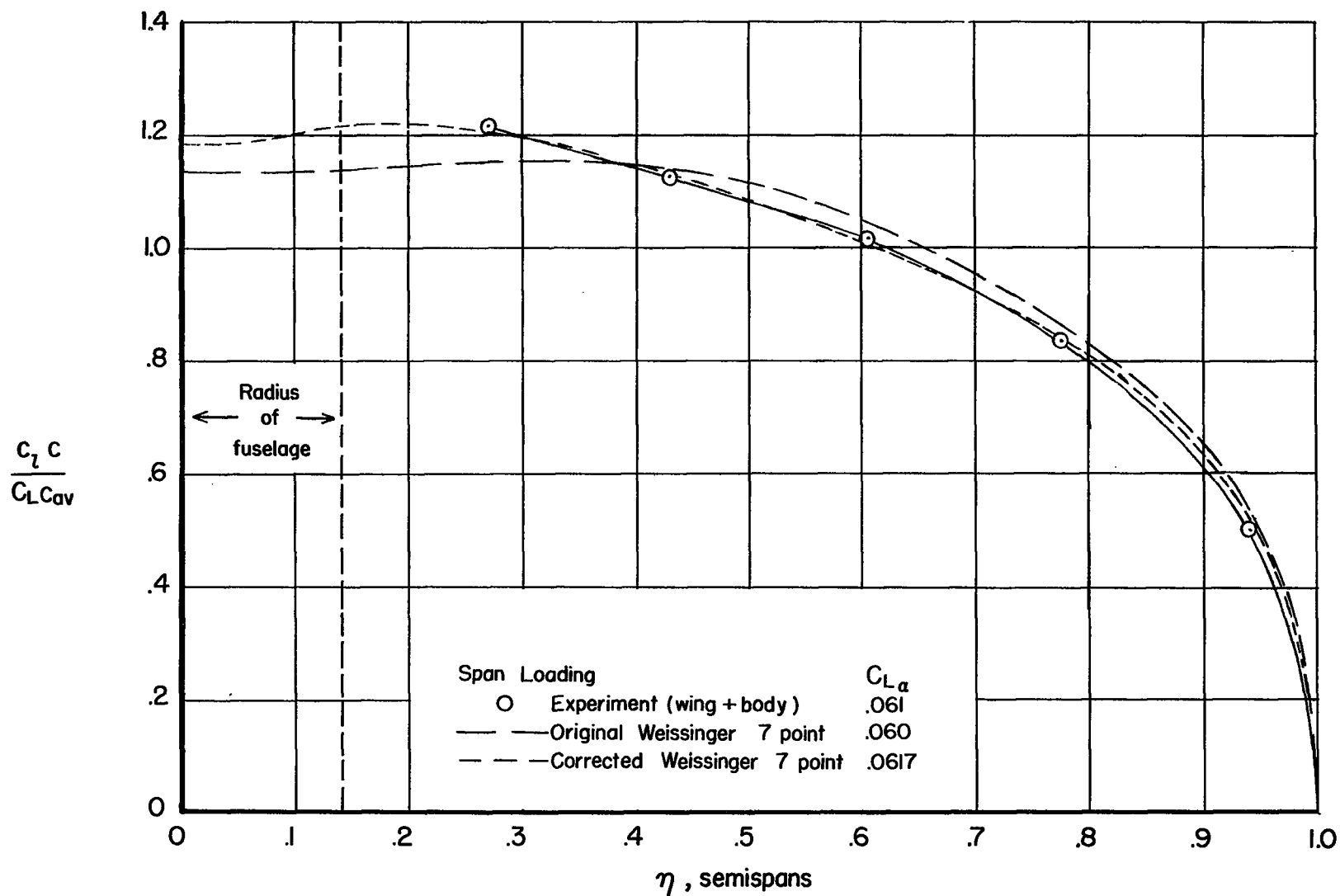
(a) $A = 10$, $\Lambda = 40^\circ$, $\lambda = 0.4$.

Figure 3.- Comparison of 7-point results with experiment.



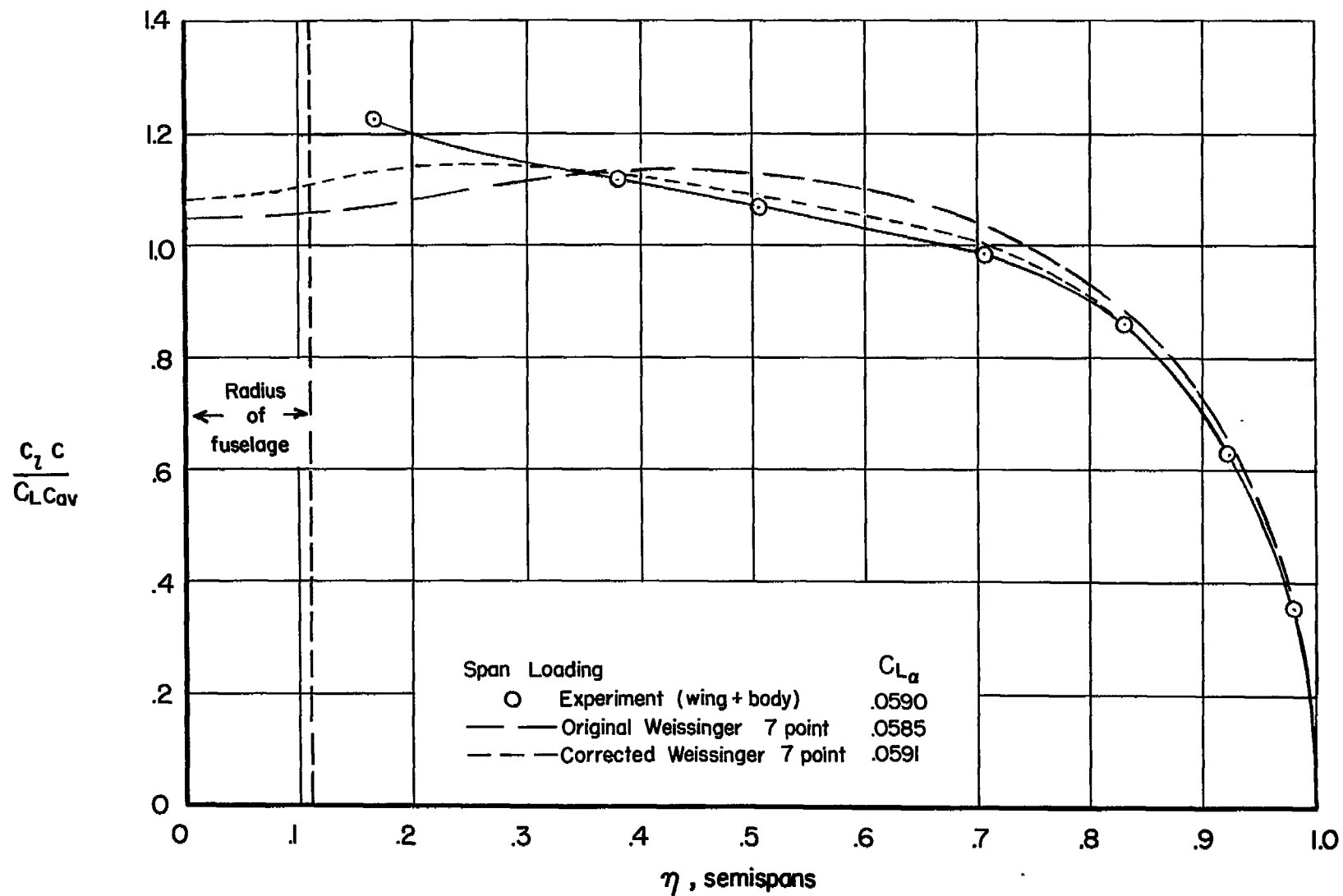
(b) $A = 8$, $\Lambda = 45^\circ$, $\lambda = 0.45$.

Figure 3.- Continued.



(c) $A = 6$, $\Lambda = 45^\circ$, $\lambda = 0.29$.

Figure 3.- Continued.



(d) $A = 6$, $\Lambda = 45^\circ$, $\lambda = 0.5$.

Figure 3.- Concluded.

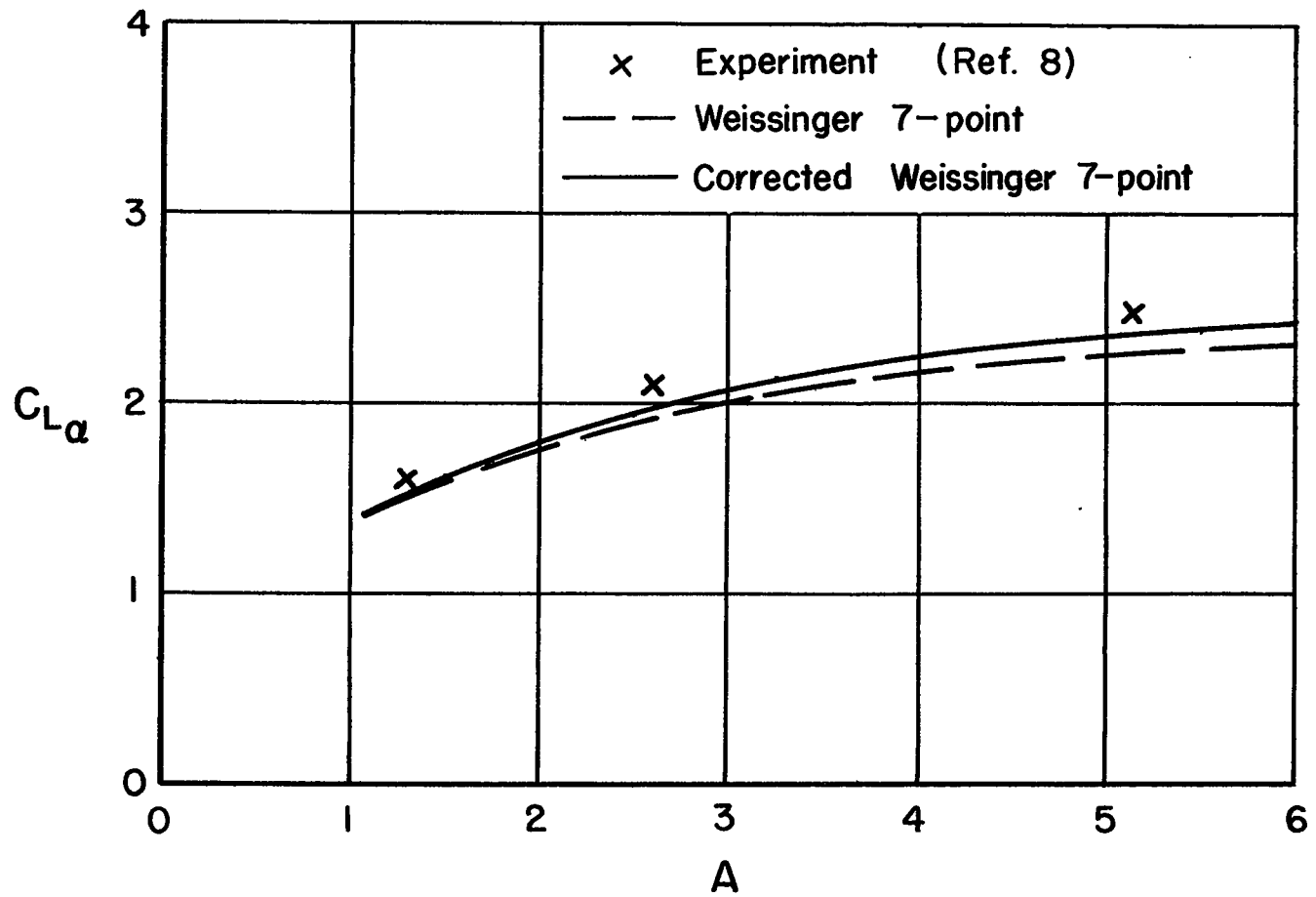


Figure 4.- Comparison of experimental lift-curve slopes with computed values;
 $\Lambda = 60^\circ$ and $\lambda = 1.0$.